Energy Proceedings
Vol 58, 2025
ISSN 2004-2965

Integrated topology optimization and microchannel cold plate for chip cooling#

Ningbo Wang [1], Bo Tian [1], Lu Liu [1], Junshan Li [2], Shuangquan Shao [1*]

1 School of Energy and Power Engineering, Huazhong University of Science and Technology, Wuhan 430074, China

2 Inspur Communication Information System Co., Ltd, Jinan, 250000, China
(Corresponding Author: shaoshq@hust.edu.cn)

ABSTRACT

To address the challenge of high heat flux chip cooling, this study proposes a novel liquid-cooled heat sink that integrates topology optimization with microchannel design. The novel proposal combines the superior flow characteristics of straight microchannels with the enhanced heat dissipation performance of topologically optimized structures. Firstly, a multi-objective topology optimization framework is developed to simultaneously minimize the average temperature and power dissipation of the cold plate, achieving a balance between thermal and hydraulic performance. Secondly, a three-dimensional numerical model is constructed based on the results of two-dimensional topology optimization, and its accuracy is validated. Finally, the performance of the proposed scheme was compared with that of the straight microchannel and separate topology optimization design. The results show that the proposed structure reduces the maximum chip temperature by 4.28 K and the pressure drop by 319.42 Pa compared with the straight microchannel, while also improving temperature uniformity. These findings demonstrate the effectiveness of the integrated scheme for designing high-performance cold plates tailored to the thermal management needs of electronic devices.

Keywords: Liquid cooled heat sink, High heat flux chip cooling, Topology optimization, Heat exchange

1. INTRODUCTION

The rapid development of cloud computing, artificial intelligence, and 5G communication technologies has significantly increased the power density of high-performance chips, placing greater demands on thermal management systems [1]. Efficient heat dissipation is now critical for maintaining the reliability, performance, and lifespan of electronic components, particularly in data centers and high-power computing environments [2]. As traditional air-cooling methods struggle to meet these rising thermal loads, liquid-cooling has gained widespread adoption for its superior heat transfer capabilities.

Extensive research has been devoted to optimizing cold plate heat sink designs through various cold channel layouts, including straight microchannels, serpentine microchannels [3], tree-shaped microchannels [4, 5], V-shaped fin structures [6], and wave-shaped microchannels [7, 8], etc. Among various liquid cooling configurations, straight microchannel heat sinks are widely studied for their structural simplicity and favorable hydraulic performance. Their stable operation and low-pressure characteristics contribute to energy-efficient cooling [9]. However, a key limitation of straight microchannels is that they cannot ensure a uniform flow distribution, especially under spatially non-uniform heat loads. This shortcoming often results in low efficiency in hotspot management, posing thermal reliability challenges in high heat flux chip applications.

Topology optimization originated from structural optimization problems [10], but has also been applied to cold plate design problems and has emerged as a powerful computational approach for the design of high-performance thermal management systems [11]. Koga et al. [12] established a comprehensive framework for applying topology optimization to heat sink design and experimentally validated its effectiveness in reducing pressure drop and enhancing heat dissipation. Similarly, Li et al. [13] introduced a topology optimization-based method for designing liquid-cooled heat sinks, demonstrating improved thermal performance through reduced thermal resistance and increased Nusselt number compared to conventional parallel-channel designs. However, despite these promising results, topology-optimized structures often exhibit high flow resistance and complex geometries, which can lead to increased pumping power requirements and manufacturing difficulties [14].

To address these limitations of conventional designs, integrated cooling designs are gaining attention as a way to combine the advantages of different cold plate

This is a paper for the 11th Applied Energy Symposium: Low Carbon Cities & Urban Energy Systems (CUE2025), July 18-22, 2024, Kitakyushu, Japan.

solutions [15]. However, limited research has explored the direct integration of topology optimization with microchannel structures within a unified design framework. In this study, we propose a novel liquid-cooled cold plate that merges topology-optimized regions with straight microchannel layouts, capitalizing on the favorable flow uniformity and low-pressure drop of microchannels alongside the enhanced heat dissipation offered by topology optimization. This integrated design offers a scalable, high-efficiency thermal management solution for high heat flux electronic systems and provides valuable design insights for future applications in electric vehicle power modules and aerospace electronics.

2. DESIGN OF COLD PLATE BASED ON TOPOLOGY OPTIMIZATION

2.1 Physical description

As illustrated in Fig. 1, the cold plate is defined as the design domain for two-dimensional topology optimization. The variable density method is employed, assuming that the design domain as a porous medium whose material properties are governed by the design variable γ. The variable γ ranges from 0 to 1, where $\gamma = 0$ represents solid material and $\gamma = 1$ corresponds to fluid regions. To achieve a balance between heat dissipation and pumping power, the optimization objective is to minimize both the average temperature of the cold plate and its power dissipation. The design domain dimensions are 14.8L in length and 12.4L in width, with an inlet width of 1.5L. The inlet temperature T_{in}^* is set to 298.15 K, and the outlet pressure P_{out}^* is fixed at 0 Pa.

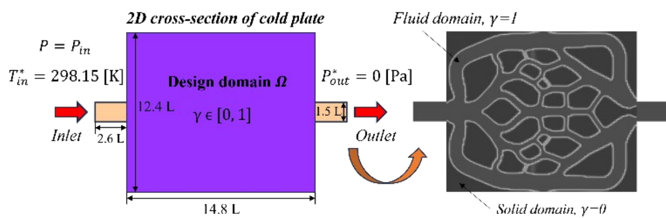

Fig. 1. Schematic of 2D topology optimization problem

2.2 Governing equation

Assuming that the coolant in the liquid cooling plate is stable and incompressible, and the Reynolds number calculations indicate that the flow is laminar. The flow equation is controlled by the following governing equation:

$$\nabla \cdot \boldsymbol{u} = 0 \tag{1}$$

$$\rho(\boldsymbol{u} \cdot \nabla)\boldsymbol{u} = -\nabla p + \mu \nabla^2 \boldsymbol{u} + \boldsymbol{F} \tag{2}$$

where $\boldsymbol{u}$ is the velocity, p and μ represent the density, pressure and viscosity, respectively. F denotes the body force, that is, the flow resistance.

Due to the distinct heat transfer mechanisms in the fluid domain and solid domain, the governing equations for energy conservation differ between the two regions. The energy equations for the fluid domain and solid domain are expressed in equations (3) and (4), respectively. To enable a unified formulation across the entire design domain, a linear interpolation of the thermal conductivities of the fluid domain and solid domain is employed. This results in a combined energy governing equation applicable to both domains, as presented in equation (5).

$$\rho c_p (\boldsymbol{u} \cdot \nabla T) = k_f \nabla^2 T \tag{3}$$

$$0 = k_s \nabla^2 T + \dot{Q} \tag{4}$$

$$\gamma \rho c_p (\boldsymbol{u} \cdot \nabla) T = \left[(1-\gamma) k_s + \gamma k_f\right] \nabla^2 T + (1-\gamma) Q \tag{5}$$

where k_s and k_f are respectively the effective thermal conductivity of solids and liquids, c_p represents the specific heat capacity, T and $\dot{Q}$ are the temperature of design domain and heat generation of solid domain, respectively.

2.3 Topology optimization process

In this study, the topology optimization design was carried out by minimizing the average temperature of the cold plate and minimizing power dissipation, thereby obtaining the solution for the coordinated improvement of heat exchange efficiency and energy consumption. The average temperature $\emptyset_T$ and power dissipation $\emptyset_f$ of the cold plate can be obtained by equations (6) and (7), respectively.

$$\phi_T = \frac{\int T d\Gamma_Q}{\int d\Gamma_Q} \tag{6}$$

$$\phi_f = \mu \int_\Omega \nabla \boldsymbol{u} \cdot \nabla \boldsymbol{u} d\Omega + \int_\Omega \alpha(\gamma) \boldsymbol{u} \cdot \boldsymbol{u} d\Omega \tag{7}$$

where Ω represents the design domain and $\boldsymbol{u}$ is the fluid velocity.

Since the magnitudes of the average temperature objective $\emptyset_T$ and the power dissipation objective $\emptyset_f$ differ significantly, this study normalizes them using reference values Φ_T^0 and Φ_f^0, respectively. The complete optimization objective is defined in equation (9), where the two normalized objectives are combined through a weighted sum. An average temperature weighting factor W_t and a power dissipation weighting

factor W_f are introduced to balance the trade-off between thermal and hydraulic performance.

$$\phi_T^n = \frac{\phi_T}{\phi_T^0}, \quad \phi_f^n = \frac{\phi_f}{\phi_f^0} \tag{8}$$

$$\phi = W_t \phi_T^n + W_f \phi_f^n \tag{9}$$

Herein, the mathematical description of the liquid cooling plate design problem based on topology optimization is as follows:

$$\begin{aligned} & find\ \gamma \\ & min\ \ \phi = W_t\phi_T^n + W_f\phi_f^n \\ & s.t. \begin{cases} 0 \le \dfrac{\int_\Omega \gamma d\Omega}{\int_\Omega d\Omega} \le \varphi_{avg} \\ 0 \le \gamma \le 1 \\ W_t + W_f = 1 \end{cases} \end{aligned} \tag{10}$$

where W_t and W_f are temperature weighting factor and power dissipation weighting factor, respectively. φ_{avg} represents the fluid volume fraction constraint, which is an aspect that needs to be studied in this paper.

The topology optimization of the liquid-cooled plate involves coupled multi-physics fields and is performed using COMSOL Multiphysics 6.3. To evaluate the impact of mesh resolution on the optimization results, four different quadrilateral mesh sizes were compared. As the mesh is refined, the resulting flow channels become more distinct and the structural features more detailed. Considering the trade-off between computational efficiency and solution accuracy, a mesh size of 0.08L was selected for all subsequent simulations in this study.

2.4 Topology optimization results

Different objective weight coefficients W_t and average fluid volume fractions φ_{avg} are an important factor affecting the topology optimization results. In this study, the topology optimization results were investigated for $\varphi_{avg} = 0.5$ when $W_t = 0.6\ and\ 0.7$, respectively. Fig. 2 illustrates the topology optimization results of cold plates under different W_t and φ_{avg}. These design structures reveal how varying the optimization priorities affects internal flow path and structural characteristics. When φ_{avg} remains unchanged, the flow channels become denser as W_t increases. When W_t is large, thermal performance is prioritized, resulting in larger flow channels and denser structures for enhanced heat transfer. As W_t decreases, the focus shifts toward hydraulic performance, producing more streamlined paths with reduced pressure drops. These results demonstrate the effectiveness of topology optimization in balancing thermal performance and power dissipation objectives, providing a promising solution for the development of high-performance cold plates suited to specific application requirements.

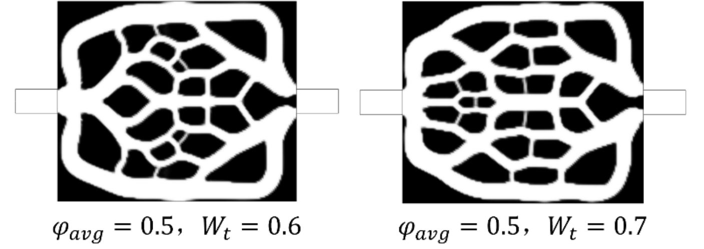

Fig. 2. Topology optimization results under different objective weighting coefficients W_t and φ_{avg}

3. NUMERICAL ANALYSIS AND VALIDATION

3.1 Three-dimensional numerical analysis model

To demonstrate the superior performance of the integrated topology optimization and straight microchannel design, a comparative study was conducted against baseline configurations: the conventional straight microchannel cold plate and the topology-optimized cold plate. As illustrated in Fig. 3, four different cold plate configurations are evaluated to investigate the influence of various structural design strategies on thermal and hydraulic performance. Case A, featuring a traditional straight microchannel structure, demonstrates low pressure drop due to its simple and regular geometry. The three-dimensional models of Case B and Case C were established based on the results of topology optimization. Case B is the topology optimization structure with $\varphi_{avg} = 0.5$ and $W_t = 0.6$, and Scheme C is the topology optimization structure with $\varphi_{avg} = 0.5$ and $W_t = 0.7$. Case B and Case C enable more adaptive flow distribution toward high heat flux regions, resulting in enhanced heat dissipation, but at the cost of increased flow resistance and structural complexity. The three-dimensional model of Case D presents a hybrid scheme that integrates topology optimization with embedded straight microchannels, which maintains the efficient flow characteristics of microchannels while leveraging the heat spreading capability of the topology-optimized pathways.

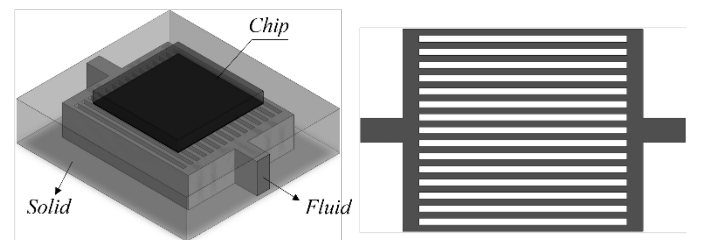

(a) Case A: Straight microchannel

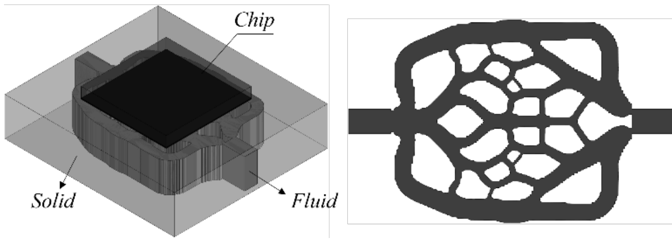

(b) Case B: Topology optimization solution ($\varphi_{avg} = 0.5$ and $W_t = 0.6$)

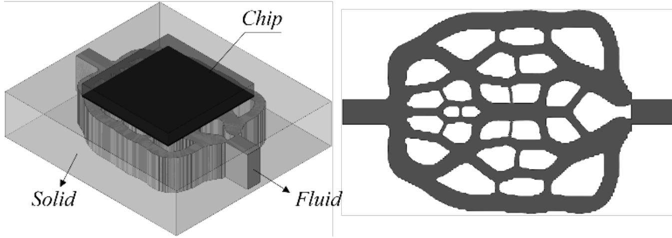

(c) Case C: Topology optimization solution ($\varphi_{avg} = 0.5$ and $W_t = 0.7$)

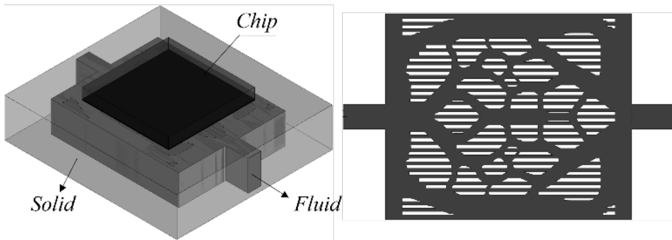

(d) Case D: Topology optimization combined with Straight microchannel

Fig. 3. Three-dimensional structure of the cold plate

3.2 Boundary conditions and grid independence tests

Three-dimensional numerical simulation was performed based on Ansys Fluent. The material properties of aluminum and water are assigned to the cold plate and coolant, respectively. Coolant is considered to be incompressible fluid with constant properties. Thermal conductivity of TIM is set to 6 $W/(m \cdot K)$. The inlet temperature and flow rate of the coolant are set to $298.15\,K$ and $0.4\,L/min$, respectively. The outlet pressure is specified as 0 Pa. A constant heat flux of $100\,W/cm^2$ is applied to the chip surface, while other surfaces exposed to surroundings are set as adiabatic surfaces.

Grid independence testing is the fundamental to ensuring the accuracy of calculation results and improving calculation speed. This study avoided low-quality meshes by refining the contact areas between the solid domain and the fluid domain. Fig. 4 shows the variation of the maximum temperature of the chip with the number of grids. Since the flow channels in Case B, Case C, and Case D are more complex than those in Case A, the number of grids increases significantly after mesh refinement. For Case A, when the number of grids exceeds 969443, fluctuations in the maximum chip temperature caused by the number of grids can be ignored. For Case B, Case C, and Case D, when the number of grids exceeds 6521346, 6478465, and 6587782, respectively, the number of grids has almost no effect on the maximum chip temperature. Without losing generality, considering the balance between calculation accuracy and calculation speed, subsequent simulations were conducted for Cases A, Case B, Case C, and Case D with grid numbers of 969443, 6521346, 6478465, and 6587782, respectively.

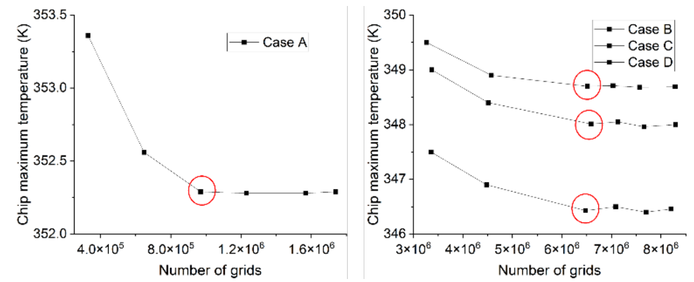

Fig. 4. The maximum temperature of the chip varies with the number of grids

3.3 Results and Discussion

Fig. 5 presents a quantitative comparison of four cold plate schemes (Cases A–D) based on several key performance indicators, including maximum and minimum temperature, temperature uniformity, thermal resistance, pressure drop, and flow resistance coefficient. In Case A, the maximum temperature of the chip reaches 352.29 K, while Case C achieves the lowest maximum temperature ($T_{max} = 346.43\,K$), indicating superior heat dissipation performance. Case A has the highest temperature nonuniformity ($T_{SD} = 1.97\,K$), while Case D achieves the lowest standard deviation (T_{SD} =1.20 K), indicating excellent thermal uniformity. Although Cases A and B achieve efficient heat dissipation with minimal thermal resistance, the pressure drop increases significantly. Case D achieves a pressure drop of 1415.23 Pa and has the lowest flow resistance coefficient ($f = 0.88$). Although Case A has a comparably low pressure drop, its poor thermal performance makes it unsuitable for applications in high flux devices. Overall, Case D strikes a balance between thermal efficiency and pressure loss, while offering excellent temperature uniformity and minimal flow resistance, making it ideal for practical high flux chip cooling.

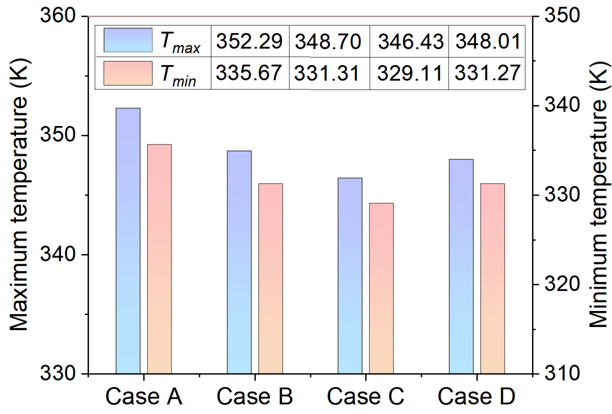

(a) Maximum temperature and minimum temperature

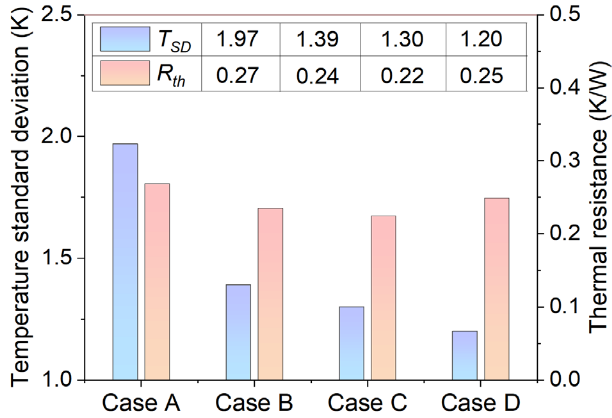

(b) Temperature standard deviation and thermal resistance

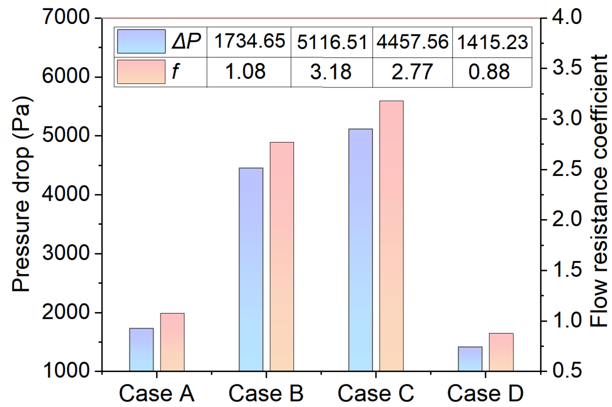

(c) Pressure drop and flow resistance coefficient

Fig. 5. Comparison of key performance indicators under different cold plate structures

4. CONCLUSIONS

This study addresses the challenges of high flux chips cooling in data centers by proposing an innovative liquid-cooled heat sink that integrates topology optimization and microchannel design. Key conclusions are summarized as follows:

(1) A multi-objective topology optimization framework, leveraging Darcy interpolation and Helmholtz filtering, effectively balances thermal performance and hydraulic efficiency. Parametric studies reveal that thermal weighting coefficients (W_t) critically influence flow path complexity and heat transfer uniformity.

(2) Compared to straight microchannels (Case A), the topology-optimized structure (Case C) reduces maximum chip temperature by 5.86 K. The integrated design (Case D) further enhances practicality, achieving a 4.28 K temperature reduction and 319.42 Pa pressure drop reduction while improving temperature uniformity compared to straight microchannels.

This work provides a scalable strategy for designing adaptive cold plates that optimize flow distribution and heat dissipation in high power devices. Future applications could extend to electric vehicle batteries and aerospace systems where thermal management is critical.

ACKNOWLEDGEMENT

This work was supported by the program for HUST Academic Frontier Youth Team (No.2019QYTD10) and the Fundamental Research Funds for the Central Universities, HUST (2024JYCXJJ046).

REFERENCE

[1] N. Wang, Y. Guo, C. Huang, S. Shao. Advances in direct liquid cooling technology and waste heat recovery for data center: A state-of-the-art review. Journal of Cleaner Production. 477 (2024) 143872.

[2] N.G. Patil, T.K. Hotta. A Combined Liquid Cold Plate and Heat Sink Based Hybrid Cooling Approach for the Temperature Control of Integrated Circuit Chips. Journal of Thermal Science and Engineering Applications. 14 (2022).

[3] N. Wang, C. Li, W. Li, X. Chen, Y. Li, D. Qi. Heat dissipation optimization for a serpentine liquid cooling battery thermal management system: An application of surrogate assisted approach. Journal of Energy Storage. 40 (2021) 102771.

[4] O. Yenigun, E. Cetkin. Experimental and numerical investigation of constructal vascular channels for self-cooling: Parallel channels, tree-shaped and hybrid designs. International Journal of Heat and Mass Transfer. 103 (2016) 1155-65.

[5] Y. Xu, W. Zhang, Y. Li, P. Lu, Y. Wang, Z.S. Wu. The Synergetic Effect of Ni and Fe Bi-metal Single Atom Catalysts on Graphene for Highly Efficient Oxygen Evolution Reaction. Frontiers in Materials. 6 (2019).

[6] A.F. Al-Neama, Z. Khatir, N. Kapur, J. Summers, H.M. Thompson. An experimental and numerical investigation

of chevron fin structures in serpentine minichannel heat sinks. International Journal of Heat and Mass Transfer. 120 (2018) 1213-28.
[7] L. Lin, J. Zhao, G. Lu, X.D. Wang, W.M. Yan. Heat transfer enhancement in microchannel heat sink by wavy channel with changing wavelength/amplitude. International Journal of Thermal Sciences. 118 (2017) 423-34.
[8] J. Zhou, M. Hatami, D. Song, D. Jing. Design of microchannel heat sink with wavy channel and its time-efficient optimization with combined RSM and FVM methods. International Journal of Heat and Mass Transfer. 103 (2016) 715-24.
[9] K. Monika, S.P. Datta. Comparative assessment among several channel designs with constant volume for cooling of pouch-type battery module. Energy Conversion and Management. 251 (2022) 114936.
[10] M.P. Bendsøe, N. Kikuchi. Generating optimal topologies in structural design using a homogenization method. Computer Methods in Applied Mechanics and Engineering. 71 (1988) 197-224.
[11] P. Chen, L. Gao, W. Li, J. Zhao, A. Garg, B. Panda. A topology optimization-based-novel design and comprehensive thermal analysis of a cylindrical battery liquid cooling plate. Applied Thermal Engineering. 252 (2024) 123747.
[12] A.A. Koga, E.C.C. Lopes, H.F. Villa Nova, C.R.d. Lima, E.C.N. Silva. Development of heat sink device by using topology optimization. International Journal of Heat and Mass Transfer. 64 (2013) 759-72.
[13] H. Li, X. Ding, F. Meng, D. Jing, M. Xiong. Optimal design and thermal modelling for liquid-cooled heat sink based on multi-objective topology optimization: An experimental and numerical study. International Journal of Heat and Mass Transfer. 144 (2019) 118638.
[14] D. Martínez-Maradiaga, A. Damonte, A. Manzo, J.H.K. Haertel, K. Engelbrecht. Design and testing of topology optimized heat sinks for a tablet. International Journal of Heat and Mass Transfer. 142 (2019) 118429.
[15] X.-h. Han, H.-l. Liu, G. Xie, L. Sang, J. Zhou. Topology optimization for spider web heat sinks for electronic cooling. Applied Thermal Engineering. 195 (2021) 117154.